Observing and Modeling Drainage Networks from Supraglacial Lakes on Russell Glacier, West Greenland

Engineering Honors Capstone Report
Winter 2022

Student
Lydia Gilbert
University of Michigan B.S.E. Climate & Meteorology - Meteorology
Minors in Computer Science and Latin

Advisor
Professor Jeremy Bassis
Climate and Space Science and Engineering

Abstract

Formation and drainage of supraglacial lakes on the margin of the Greenland Ice Sheet (GrIS) is a crucial component of ice sheet surface ablation, development of supraglacial meltwater streams and ice dynamics. However, we don't yet understand all of the controls on the spatio-temporal patterns of lake formation and drainage. Our study aims to investigate the processes that control the patterns of supraglacial lake filling and drainage cycles over an entire melt season on a section of the western GrIS near Russell Glacier. To do this we first determined locations of lakes using Landsat visible imagery. We found that lakes first initiated at low elevation early in the melt season, before progressing to increasingly higher elevations as the melt season progressed. Over the course of the melt season, lakes at lower elevations first drained and disappeared with higher elevation lakes disappearing later in the melt season. Based on these results, we anticipate that lakes were filling, overtopping and potentially draining through moulins throughout. To test this, we developed a simple model of supraglacial lake filling and drainage driven by surface air temperature. The model routed water downstream based on the direction of steepest slope. Preliminary results from the model show that supraglacial lakes first fill at lower elevations where it is warmer. As the melt season progresses, the isotherm where melt first occurs shifts to higher elevation, as seen in the observations. However, unlike observations, the model predicts persistent lakes at lower elevation. We anticipate that is a consequence of the fact that we have not included the possibility of moulin drainage in our model.

1. Introduction

Supraglacial lakes form and drain off of the ice sheet surface via several pathways (Figure 1). They form when the sun melts the top layer of ice and snow on the ice sheet to create meltwater, which accumulates in ponds and lakes (i.e. supraglacial lakes). Once full, lakes overtop and meltwater drains off of the ice sheet through a network of channels on the ice surface. Meltwater can also drain through holes in the ice called moulins that can be deep enough to reach the bed of the ice sheet.

Supraglacial lakes and meltwater dynamics impact meltwater runoff calculations and ice dynamics in climate models and sea level rise estimates. Meltwater from the GrIS surface that drains through moulins to the bottom of the ice sheet may affect the lubrication of the GrIS (Shannon et al. 2013). The enhanced-basal meltwater lubrication may increase sea level rise through mass loss from additional iceberg calving (Shannon et al. 2013). In a warming climate consistent with RCP 4.5 and 8.5, supraglacial lakes are predicted to form further inland and cover a larger section of the GrIS (Leeson et al. 2014). Up to one half of these lakes are large enough to drain, potentially adding significant amounts of meltwater to enhance basal lubrication (Leeson et al. 2014). Supraglacial lakes are also likely to be larger in size at higher elevations under a warmer climate (Lüthje et al. 2006).

There is much we do know about supraglacial lakes and their associated processes from previous observational and modeling studies. Modeled supraglacial lakes on the GrIS overtop and drain into lakes at lower elevations, according to studies that utilized a surface energy balance model and a fluid dynamics model (Banwell et al. 2012; Kingslake et al. 2015). On the western GrIS, small lakes at low elevations were more likely to drain, large lakes at high elevations were more likely to persist into the winter, and some lakes at high elevations drained

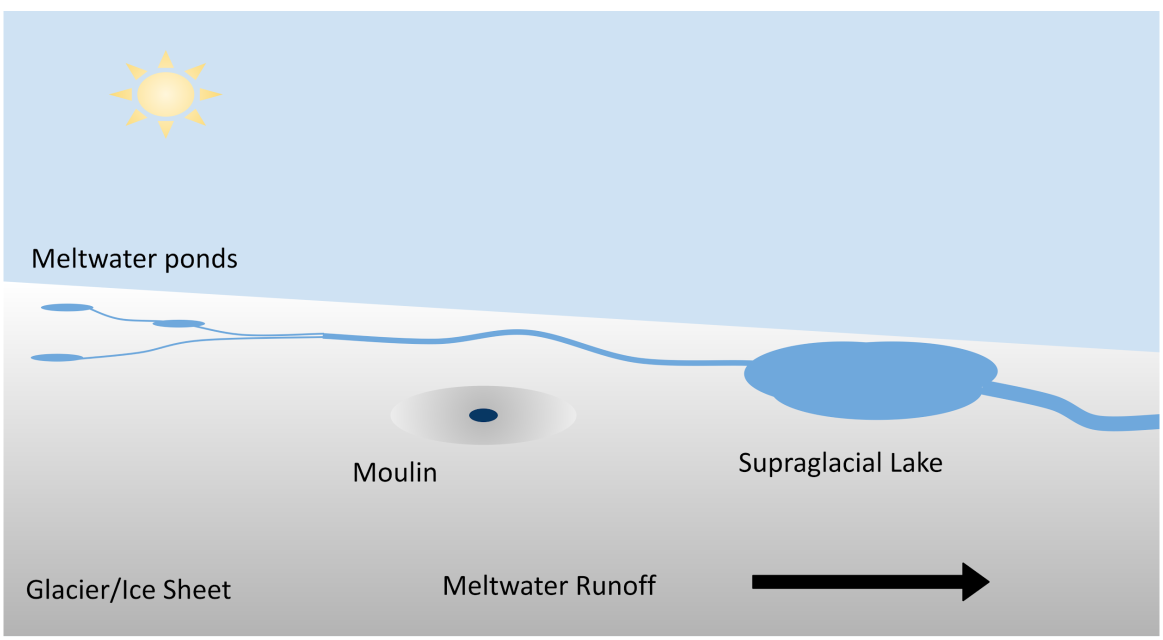

Figure 1. Conceptual model detailing supraglacial lake formation from meltwater ponds and drainage via moulins and runoff.

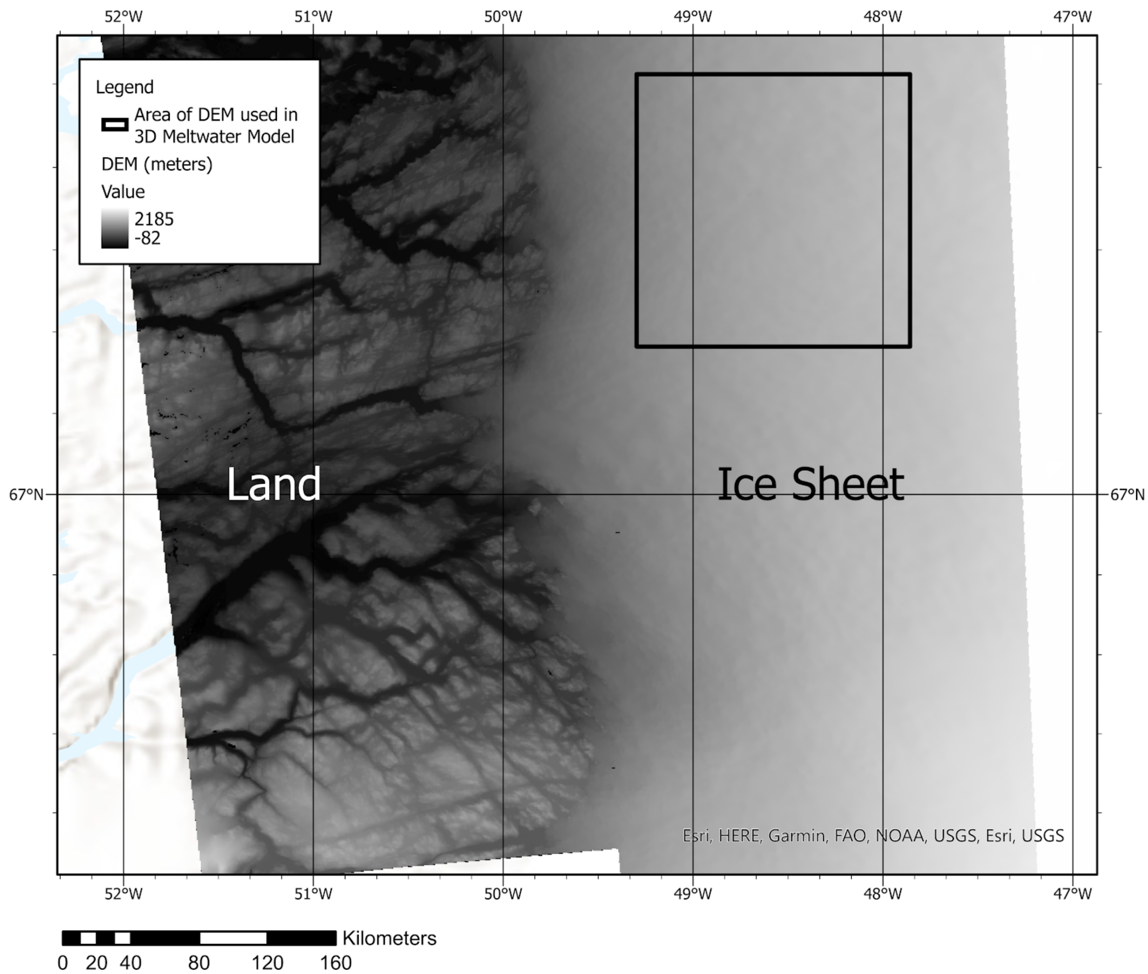

Figure 2. A map of the study area with an elevation model. The study area on the western GrIS highlighted in the bound box, covering approximately 25,000 km^2.

into moulins (Yang et al. 2021). Another study found that moulins in the GrIS form mainly as a function of rapid supraglacial lake draining (Hoffman et al. 2018). During more intense melt years, supraglacial lakes form at higher elevations, are more susceptible to moulin formation, and have shorter lifespans (Liang et al. 2012). One study found that 39% of meltwater entered the englacial system through moulins or moulins formed from hydrofracture events (Koziol et al. 2017). The same study also found that their model results showed the hydrofracture drainage at higher elevations increased during higher melt years (Koziol et al. 2017).

There is still a lot we don't know about supraglacial lakes. How do they form and change over a single melt season? How do moulins impact supraglacial lake coverage and evolution? How can we better represent meltwater dynamics in ice dynamics and climate models? This study aims to understand and predict the processes associated with supraglacial lakes by analyzing satellite observations and constructing a meltwater dynamics model for a section of the GrIS near Russell Glacier.

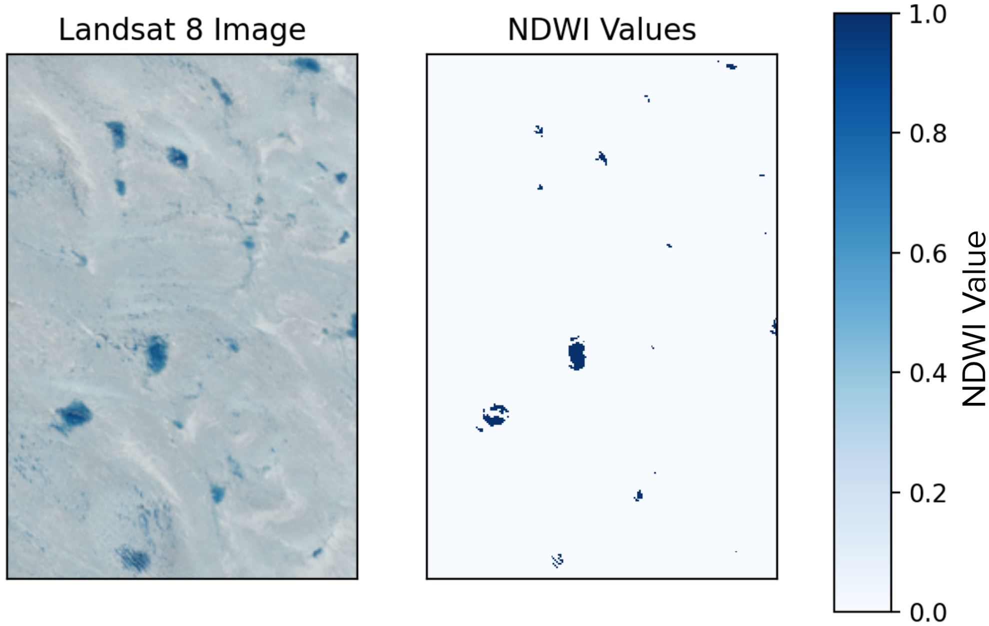

Figure 3. A section of Landsat 8 imagery compared with its corresponding calculated NDWI values. The NDWI identifies lakes shown in the Landsat 8 image fairly well.

2. Methods

a. Study Site

The area of study we selected is a section of the ice sheet east of Russell Glacier, GrIS, as seen in Figure 2. All observations come from within this domain, which the meltwater model also used as its domain. This area covers approximately 25,000 km^2 of the GrIS and has an elevation range between 1099 and 1637 meters. The annual ice velocity data from MEaSUREs for 2017 and 2018 suggested that the ice velocities do not exceed 90 meters per year in the study area, such that we ignored ice sheet movement in our study of the 2019 melt season (Joughin 2020). In June 2019, we were in Greenland near Russell Glacier as part of a research expedition to provide undergraduate students with field research experience (Snide et al. 2020). We chose this study site because we were inspired by our experiences there to start this project.

b. Datasets

We used several datasets in our observational analysis and modeling process. Observations of supraglacial lakes were derived from Landsat 8 imagery with minimal cloud coverage and a resolution of 30 meters. The dates of images were May 9, June 10, July 12, and August 13, 2019. We focused on the 2019 melt season (May to August) because it was the only year there was a suitable Landsat 8 image from each month of the melt season. We also happened to be in Greenland in June of 2019 and observed the glacial runoff from the mid-June melt event in the glacial rivers near Kangerlussuaq, Greenland. ArcticDEM, a digital elevation model (DEM) published in 2018, was the proxy for ice sheet topography and elevation and had a resolution of 32 meters, comparable to the Landsat 8 imagery (Porter et al. 2018). Daily surface air temperature data came from the ERA5 reanalysis data and was on a 0.25°x0.25° grid (C3S 2017).

c. Observation Processing

We separated supraglacial lakes from ice in the Landsat8 imagery with an index called the Modified Normalized Difference Water Index (NDWI) (Xu 2005).

$$MNDWI = \frac{Green - SWIR}{Green + SWIR} \quad (1)$$

In Equation 1, Green corresponds to Landsat 8 Band 3 (0.533-0.590 µm) and SWIR corresponds to Landsat 8 Band 6 (1.566-1.651 µm). Cells with NDWI values above 0.5 were classified as lakes and cells below 0.5 were classified as ice. Figure 3 shows a comparison between Landsat 8 visible imagery and classified NDWI values for a section of the GrIS. The NDWI approximated supraglacial lake locations from the Landsat 8 images fairly well. The rasters resulting from the NDWI classification served as the dataset of observed supraglacial lakes for this study.

In ArcGIS, we calculated the mean lake elevation and lake area for each lake from the DEM and NDWI rasters. We also calculated the mean cumulative Positive Degree Day (PDD) for each lake. The cumulative PDD is the sum of the daily average temperature above 0°C for a given time range.

$$PDD = \int_{t1}^{t2} T - 273.15\, dt \quad (2)$$

In Equation 2, the integral bounds t1 and t2 represent the time range for which the PDD is calculated and T represents the daily mean surface air temperature in Kelvin. For the observations, t1 was May 1, 2019, t2 was the observation date, and T came from the ERA5 reanalysis data. We further processed observed lakes, sorting them by mean elevation into bins with a width of 50 meters. The range of the bins was from 1100 meters to 1650 meters. Then we calculated the mean of all the mean elevations, the mean of all mean PDDs, and the sum of all areas of the lakes in each bin.

We performed validation on the ERA5 surface air temperature and DEM data. Lapse rates calculated from mean lake elevation and mean lake air temperature had values near the dry adiabatic lapse rate of 9.8 K/m, which is what we expected given the low levels of moisture in Greenland. Most observed lakes also matched depressions in the DEM, indicating that the DEM is a good approximation of where lakes will form during the 2019 melt season.

d. Meltwater Model

We programmed a 3D meltwater dynamics model in Python to simulate meltwater for the 2019 melt season. The meltwater model added meltwater to each cell at the beginning of a timestep. At the beginning of an iteration, the model sorted all cells by their elevation (not

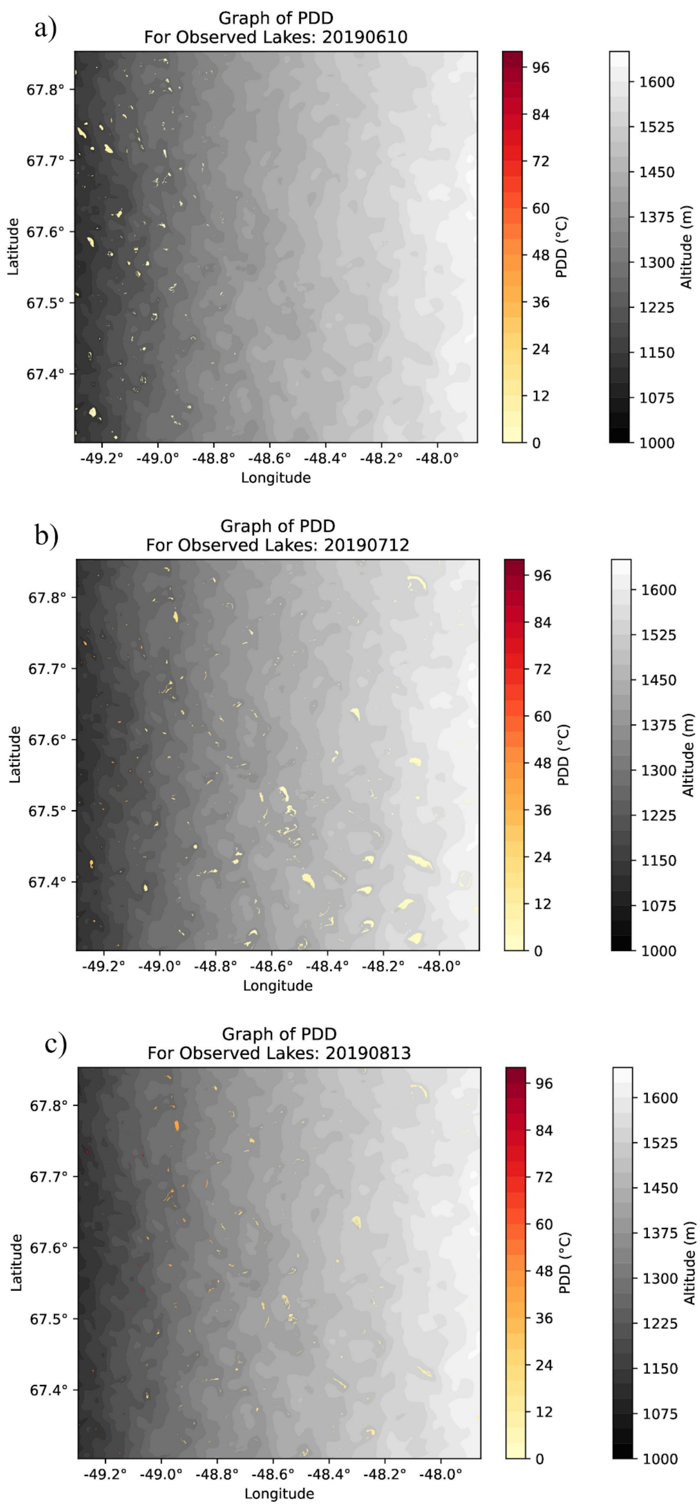

Figure 4. Maps of observed lakes overlaid with cumulative PDD for the dates (top to bottom) June 10 (a), July 12 (b) , and August 13 (c) of 2019. There was only one lake in the domain for May 9, so it is not shown here.

including water height). The model started moving water from the highest cell, then proceeded to the second highest and so on. During an iteration, water could only move to an adjacent cell, stay in the original cell, or split the amount of water between the two. Adjacent cells included the cells abutting the four sides of the original cell and the four cells diagonal to the original cell. Water flowed from the original cell to the adjacent cell with the steepest downward slope from the original cell. If the steepest downward slope was uphill or flat, the water pooled and did not move from the original cell. The slope was calculated by dividing the difference in height, which was the ice sheet elevation of the cell plus the height of the water on the cell from the previous iteration, between the original cell and an adjacent cell, divided by the distance between the two cell centers. The amount of water that moved was determined by the difference d, which was half the height difference between the original cell and the adjacent cell where the water will be moved. If the amount of the water in the original cell w, was less than d, then w amount of water moved to the adjacent cell. If $w > d$, d amount of water moved to the adjacent cell and w-d amount of water remained in the original cell. At the boundaries of the model domain, all water flowed off of the edge cell. The meltwater model continued to iterate within a timestep, moving water only once each iteration, until it reached steady state. Then the model moved on to the next timestep. Steady state was when the largest absolute difference in water height for all cells between the current iteration and previous iteration was less than a set steady state threshold. We wanted to have the steady state threshold be close to the vertical uncertainty for the elevation model, but any value smaller than 5 meters increased the model runtime too much, such that a model run could not be completed in a reasonable amount of time. The timestep for the model was one day. There was also no code for moulin behavior in the meltwater model.

The input data was an elevation model to represent the ice sheet and approximated meltwater rasters (m/day for each cell). The DEM represented the ice sheet elevation and did not change over the course of the simulation because we did not factor erosion into the meltwater model. Since the DEM was our elevation model, we set the resolution of the meltwater model at 30 meters to match the DEM. We calculated the meltwater added to each cell per day from an approximation that used PDDs (Ice Sheet System Model: Positive Degree Day).

We ran the model with a 5 meter steady state threshold between May 1, 2019 and August 31, 2019. To identify supraglacial lakes from streams and noise in the model output, any cells with water below 2 meters were classified as “ice” and cells with water above 2 meters were “lake.” We ran the binary “lake”/”ice” grids for the days of the observations through a breadth-first search to find the area, mean elevation, and mean PDD of the modeled lakes. We also ran the modeled lakes through the same binning process, with the same bin bounds, as the observed lakes.

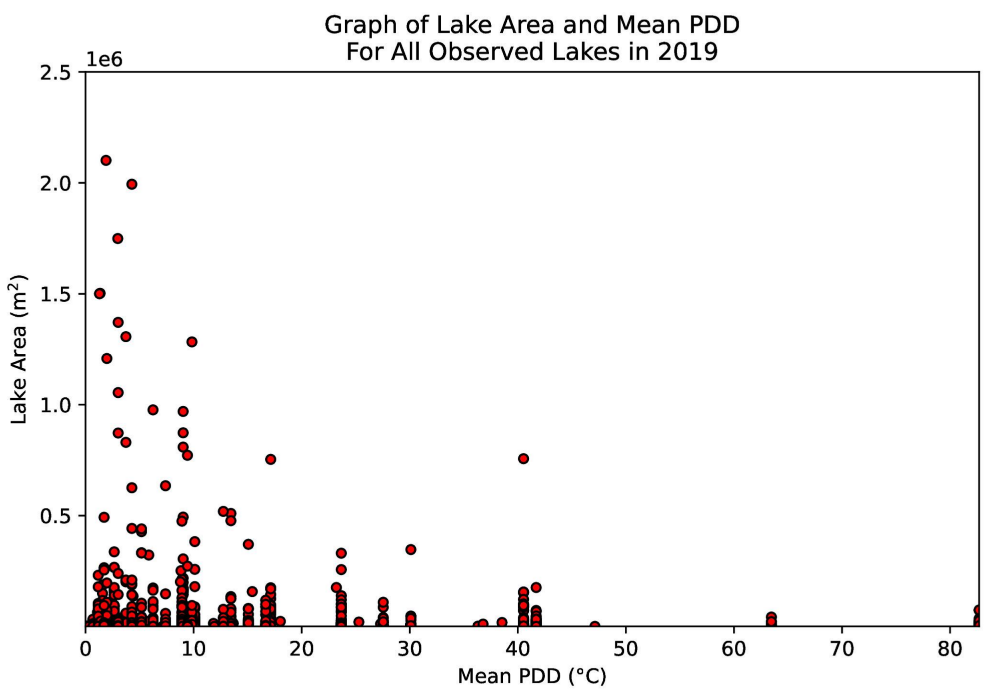

Figure 5. Lake area vs mean cumulative PDD for observed lakes, with all four dates (May 9, June 10, July 12, and August 13 of 2019) plotted on the same graph.

3. Results

a. Observations

We first looked at the spatial evolution of observed supraglacial lakes throughout the 2019 melt season. Figure 4 shows observed lakes for June 10, July 12, and August 13 with cumulative PDD overlaid. Lakes formed at low elevations early in the melt season and formed at increasingly higher elevations as the season progressed. Part way through the melt season, lakes at low elevations shrank in size and number and did not change much for the rest of the melt season (Figure 4b). Late in the melt season, observed lakes at high elevations decreased in size and number (Figure 4c). The spatio-temporal pattern observed in supraglacial lake formation is reasonable because the average air temperature increases as the melt season progresses, becoming hot enough at high elevations late in the melt season to generate melt there.

We then examined the relationship between lake area and PDDs. A low PDD value indicates that an area has not experienced many days with above freezing temperatures or has experienced a few days with temperatures well above freezing. A high PDD value indicates that an area has experienced many days with above freezing temperatures. In Figure 5, areas for observed lakes on all four dates (May 9, June 10, July 12, and August 13 of 2019) are graphed

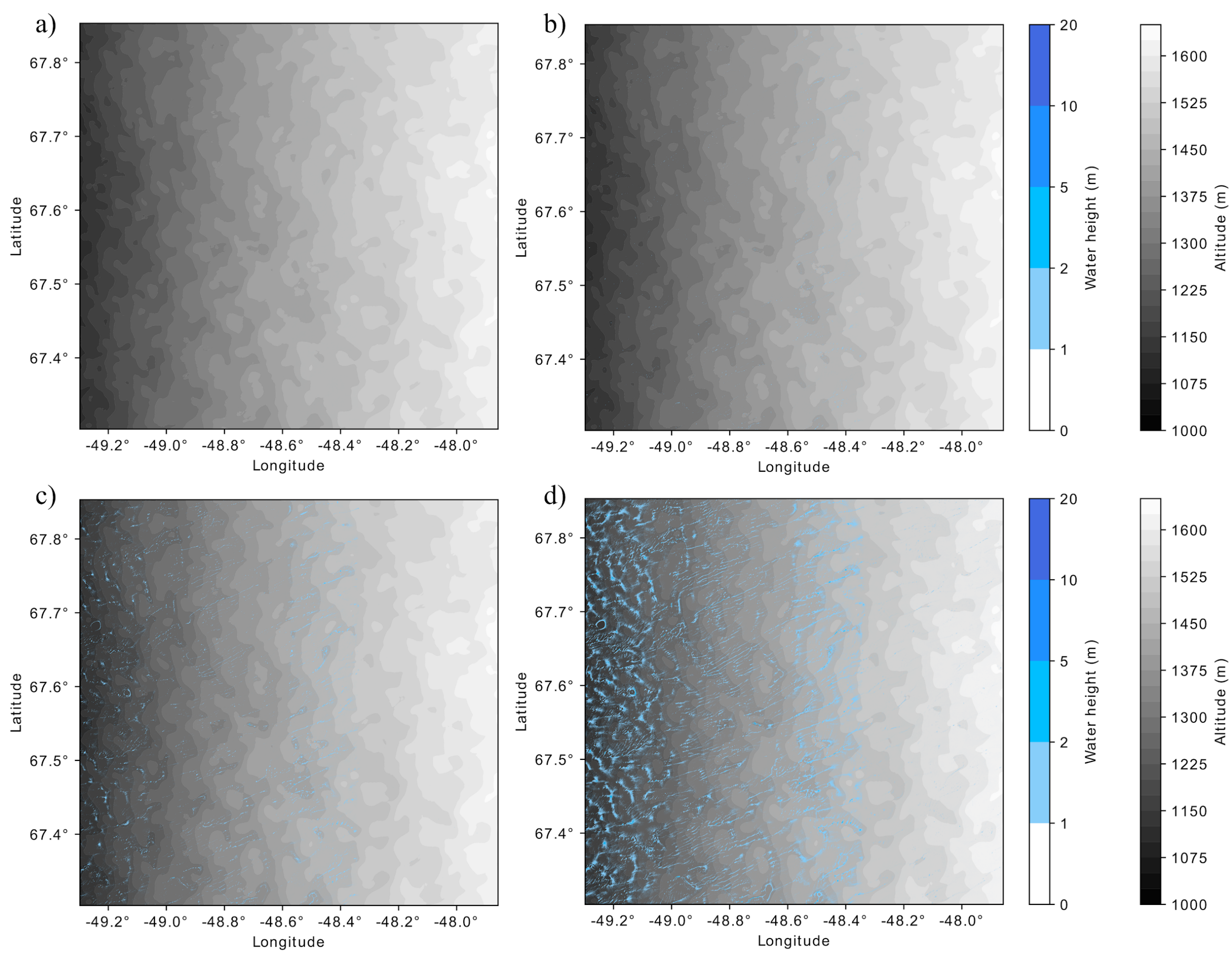

Figure 6. Maps of modeled meltwater water for the dates (a) May 9, (b) June 10, (c) July 12, and (d) August 13, 2019.

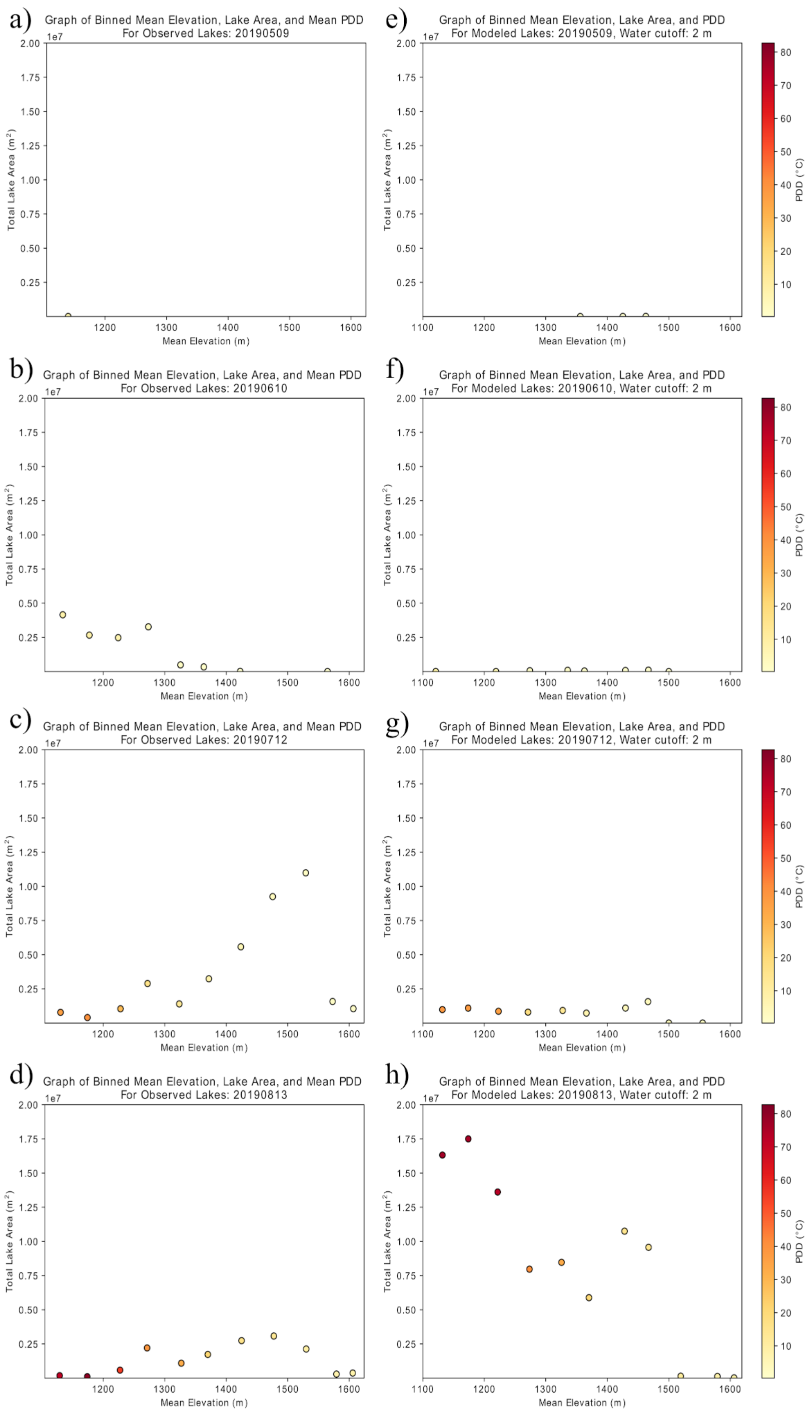

Figure 7. Total lake area vs mean lake elevation overlaid with mean cumulative PDD for observed lakes, binned by mean lake elevation (50 m width) for the dates (top to bottom) May 9, June 10, July 12, and August 13 of 2019. (e-h) Total lake area vs mean lake elevation overlaid with mean cumulative PDD for modeled lakes (water depth above 2 m), binned by mean lake elevation (50 m width) for the same dates (top to bottom) as the observed lakes.

against their mean cumulative PDD value. We define the lake zone as the region in the domain of a given observation where lakes are located. Lakes with low PDD values, likely newly formed lakes, are large and are on the eastern edge of the lake zone. Lakes with high PDD values, likely older lakes, are smaller and on the western edge of the lake zone. Large lakes only had low PDD values (~0°C - 20°C PDD), but small lakes had a large range of PDD values (~0°C - 84°C PDD). Cumulative PDDs are correlated to the elevation lakes form at and how large they grow.

b. Modeling

The simulation results show that lakes fill, overtop, and drain down off of the ice sheet. Figure 6 shows snapshots from the model simulation of meltwater height on the same days as the observations (May 9, June 10, July 12, and August 13, 2019). In the model results, lakes start to form at lower elevations, and begin to form at higher elevations and drain downhill as the melt season progresses (Figure 6). The end result is two large groups of lakes within the model domain, one at low elevation and the other at high elevations. The simulation is also fairly noisy throughout.

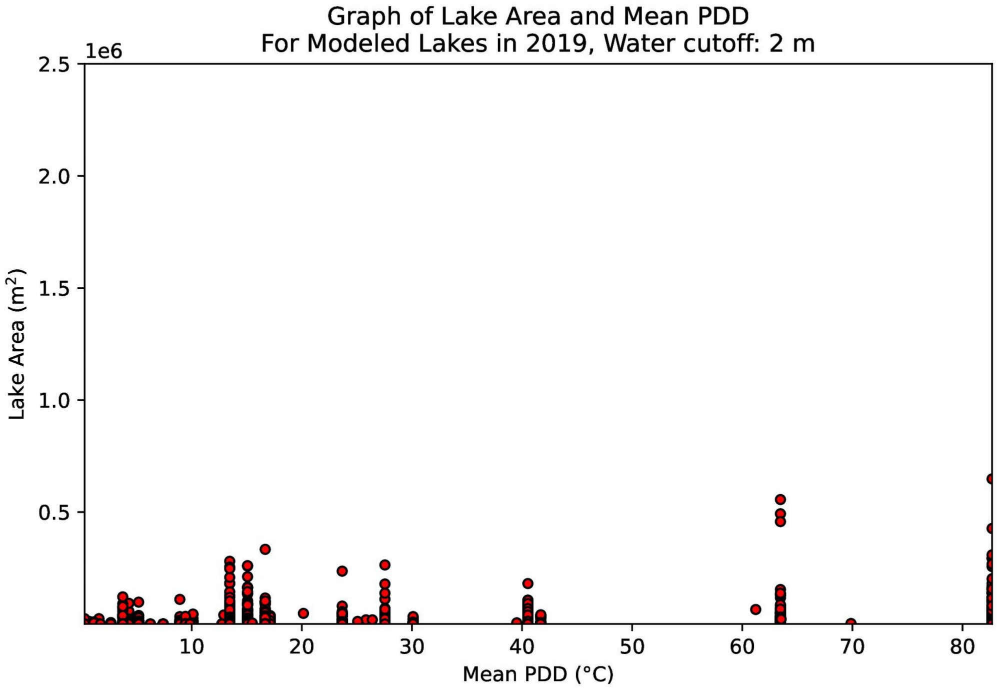

Figure 8. Lake area vs mean cumulative PDD for modeled lakes, with all four dates (May 9, June 10, July 12, and August 13 of 2019) plotted on the same graph.

The meltwater model reproduces some, but not all, of the features of the observed trends in supraglacial lake evolution. The meltwater model on the same days as the observations generally has more water on the ice sheet (Figure 6). Figure 7 presents observed and modeled lakes binned and averaged by lake elevation, with mean lake elevation on the x-axis, total lake area on the y-axis, and mean PDD overlaid. Early in the melt season, in the months of May and June, there are far more lakes and lake area than there were on the observations. At lower elevations, lakes had smaller areas than those of observed lakes. In the middle of the melt season, there are far fewer lakes at all elevations than in the observations. However, the distribution of modeled lake elevation and lake area is roughly the same, despite that the largest modeled lake was smaller than the largest observed lake. Late in the melt season, there are far more and larger modeled lakes at low elevations than in the observations.

Then we looked at the relationship between modeled lake area and mean PDD. In Figure 8, lake area is graphed against mean PDD for all modeled lakes on the dates (May 9, June 10, July 12, and August 13, 2019). Lakes with low PDD values are small and located on the eastern edge of the lake zone. Lakes with high PDD values have a large range of areas and are located on the western edge of the lake zone. Cumulative PDDs are somewhat correlated to the elevation modeled lakes formatted at and how large they grew. The meltwater model, with draining as the only mechanism for meltwater removal from the ice sheet, captured some but not all of the spatio-temporal pattern of the observed supraglacial lakes.

4. Discussion

a. Limitations

Several of the datasets we used to represent the observed lakes and physical quantities in the model have limitations. The ArcticDEM was released in 2018, but the data for the DEM was collected between 2016 and 2018 (Porter et al. 2018). Therefore the DEM is not the most accurate representation of the surface of the ice sheet before the 2019 melt season. The ArcticDEM also has the appearance of a step function, when looking at a zoomed-in slice, so water pooled very easily on these steps. This led to the fingerprint-like pattern we observed on the 2D model output maps (Figure 6). The ERA5 dataset we used a representation of air temperature and to calculate PDD has a very coarse resolution compared to the ArcticDEM and Landsat 8 resolution. This discrepancy means that the ERA5 dataset could not resolve the mean temperature over modeled and observed lakes well.

We made several assumptions in the course of this study that have impacts on our results and the interpretation of those results. We assumed that the NDWI accurately represented the locations of observed supraglacial. Although the NDWI does a fairly good job, it was not perfect and sometimes miscategorized water as ice (Figure 3). The resolution of the observations was coarse enough that the NDWI ignored glacial rivers and streams. Similarly for the meltwater model, we filtered the output water heights to focus on supraglacial lakes and remove noise by classifying any cell with a water depth above 2 meters as a lake and below 2 meters as ice. This classification method may have missed some cells that had shallow lakes or split one modeled lake into several. Additionally, we did not factor erosion into the meltwater model, so we did not account for any ice that fragmented off or eroded away and contributed to the amount of meltwater on the ice sheet. For the PDD-approximated meltwater, we only used the part of the approximation that described the melt of ice as a function of PDD and did not use the melt parameters for snow or the amount of melted snow that refroze. As a result, we may have not added enough meltwater to the model than there should have been. Since the PDD approximation also depended on the ERA5 data, it had a very coarse resolution and couldn't resolve features as small as supraglacial lakes.

b. Implications

As the melt season progresses, observed supraglacial lakes form at increasingly higher elevations, until the peak of the melt season has passed. Once new lakes reach a large enough size, they seem to shrink or disappear entirely. Older lakes at lower elevations are smaller or non-existent on satellite imagery once new lakes form. After the peak of the season in July, the size and number of lakes at high elevation also decreased. Either runoff or moulins (or both) are responsible for the reduction in observed supraglacial area and number.

The meltwater model with forcing from the PDD approximation is mostly consistent with the observations on lake formation elevation. The model result from July 12, 2019 underestimates the observed lake coverage at high elevations and the model result from August

13, 2019 grossly overestimates the observed lake coverage at low and middle elevations. Otherwise, the formation elevation is consistent between the model and observations.

The meltwater model overestimated the supraglacial lake coverage at low elevations, except early in the melt season. The meltwater model results were consistent with previous studies that show supraglacial lakes on the GrIS overtop and drain to lower elevations (Banwell et al. 2012; Kingslake et al. 2015). We think the overestimation of lake area is because of the overtopping and runoff to lower elevations, but without an additional mechanism to remove meltwater from the GrIS at lower elevations, it accumulated at the end of the melt season. We also think this mechanism is moulins that form when lakes become too large and drain the water to the bottom of the ice sheet. The relationship between observed lake area and mean PDD supports this conclusion by showing that only observed large lakes have little exposure to above freezing temperatures. The meltwater model shows that the control mechanism on the lake area-PDD relationship is not solely runoff, as it does not reproduce the relationship at all. Moulins partly control lake area and distribution on the GrIS by shrinking the area of new lakes that have grown too large.

The meltwater model captured some of the spatio-temporal pattern of supraglacial lakes, therefore another mechanism besides runoff must be responsible for removal of water from the GrIS. Moulins are likely that other mechanism and scientists must account for them in model parameterizations. Meltwater dynamics models are incomplete if they only have runoff as the only mechanism to remove water from the ice sheet.

Observed lakes showed a positive correlation between maximum positive cumulative PDD and the elevation with the largest total lake area. This indicates that higher cumulative PDDs from higher air temperatures would likely result in supraglacial lakes forming higher up on the GrIS, consistent with Leeson et al. (2014). Results from the observational and model analysis suggest that moulins are a critical component of meltwater drainage off of the ice sheet and reduction in supraglacial lake area. Meltwater runoff calculations cannot assume that all meltwater formed on the iee sheet will run off into glacier-fed streams. Some significant portion will enter the englacial system and may not exit on the same time scale as meltwater runoff calculations (Koziol et al. 2017). Meltwater that reaches the bed from moulins can contribute to enhanced basal lubrication and increased calving (Shannon et al. 2013). Climate models need to account for supraglacial lake formation and both meltwater runoff and moulins if they want to accurately predict contributions to sea level rise contributions from ice sheets.

c. Future Work

The results from the meltwater model, with runoff only, pose the questions of how including moulin behavior would the model results and moulins should be parameterized in models. We would also like to make several other steps to improve representations of physical quantities and processes in the meltwater model. Next steps from this study would include improving the representation of meltwater, adding moulins to the model, and expanding the time frame over which we ran the model. In order to improve meltwater representation, we would find a higher resolution temperature dataset and include the snow and melt refreezing parameterizations in the PDD approximation. We would also like to include moulins in the meltwater model to see if it reduces the lake area at lower elevations late in the melt season, and overall, improves the accuracy of the model. We would start with a simple parameterization of moulins, either placing them randomly or once the water height on a call had reached a threshold value. Finally, we would run the meltwater model on more than one melt season. We would need to find more supraglacial lake observations as model validation first before that happened.

5. Conclusion

Supraglacial lakes form and drain off the GrIS surface via overtopping and runoff and moulins. From the observations, we learned that lakes form at low elevations early in the melt season and form at increasingly higher elevations as the season progresses and the amount of time above freezing increases. Once new lakes reach a large enough size, they seem to shrink or disappear entirely, likely due to moulins forming. The meltwater model we constructed to reproduce these observations consistently overestimated the supraglacial lake coverage at low elevations. However, the model had runoff as the only meltwater mechanism and showed that the control on spatio-temporal patterns of supraglacial lake area and elevation is not solely runoff. From the observations and model results, we can conclude that moulins are an important part of meltwater removal from the GrIS. Future work should involve adding moulin parameterization to observe how that changes the meltwater model results.

Acknowledgments

DEMs provided by the Polar Geospatial Center under NSF-OPP awards 1043681, 1559691, and 1542736. Geospatial support for this work provided by the Polar Geospatial Center under NSF awards 1043681 and 1559691. Landsat 8 data available from the U.S.Geological Survey. Thank you to Jeremy Bassis for his enthusiasm and mentorship on this project.

References

Banwell, A. F., Arnold, N. S., Willis, I. C., Tedesco, M., and Ahlstrøm, A. P. (2012). Modeling supraglacial water routing and lake filling on the Greenland Ice Sheet. *Journal of Geophysical Research*, 117, F04012. doi:10.1029/2012JF002393.

Carrivick, J. L., Tweed, F. S., Ng, F., Quincey, D. J., Mallalieu, J., Ingeman-Nielsen, T., Mikkelsen, A. B., Palmer, S. J., Yde, J. C., Homer, R., Russell, A. J. and Hubbard, A. (2017). Ice-Dammed Lake Drainage Evolution at Russell Glacier, West Greenland. *Frontiers in Earth Science*, 5. doi:10.3389/feart.2017.00100.

Copernicus Climate Change Service (C3S) (2017): ERA5: Fifth generation of ECMWF atmospheric reanalyses of the global climate . Copernicus Climate Change Service

Climate Data Store (CDS), August 25, 2021. https://cds.climate.copernicus.eu/cdsapp#!/home.

Hoffman, M. J., Perego, M., Andrews, L. C., Price, S. F., Neumann, T. A., Johnson, J. V., and Lüthi, M. P. (2018). Widespread moulin formation during supraglacial lake drainages in Greenland. *Geophysical Research Letters*, 45, 778–788. doi:10.1002/2017GL075659.

Ice Sheet System Model: Positive Degree Day (PDD). Retrieved November 18, 2020, from https://issm.jpl.nasa.gov/documentation/pdd/.

Joughin, I. (2010). Greenland Flow Variability from Ice-Sheet-Wide Velocity Mapping. *Journal of Glaciology*, 56, 415-430. doi:10.3189/002214310792447734.

Joughin, I. (2021). *MEaSUREs Greenland Annual Ice Sheet Velocity Mosaics from SAR and Landsat, Version 3*. Annual Ice Sheet Velocities (2017-2018). Boulder, Colorado USA. NASA National Snow and Ice Data Center Distributed Active Archive Center. doi:10.5067/C2GFA20CXUI4. September 3, 2021.

Kingslake, J., Ng, F., and Sole, A. (2015). Modelling channelized surface drainage of supraglacial lakes. *Journal of Glaciology, 61*(225), 185-199. doi:10.3189/2015JoG14J158.

Koziol, C., Arnold N., Pope, A., and Colgan, W. (2017). Quantifying supraglacial meltwater pathways in the Paakitsoq region, West Greenland. *Journal of Glaciology, 63*(239), 464-476. doi:10.1017/jog.2017.5.

Leeson, A., Shepherd, A., Briggs, K. *et al.* (2015). Supraglacial lakes on the Greenland ice sheet advance inland under warming climate. *Nature Climate Change*, 5, 51–55. doi:10.1038/nclimate2463.

Liang, Y.-L., Colgan, W., Lv, Q., Steffen, K., Abdalati, W., Stroeve, J., Gallaher, D., and Bayou, N. (2012). A decadal investigation of supraglacial lakes in West Greenland using a fully automatic detection and tracking algorithm. *Remote Sensing of Environment*, 123, 127-138. doi:10.1016/j.rse.2012.03.020.

Lüthje, M., Pedersen, L., Reeh, N., and Greuell, W. (2006). Modelling the evolution of supraglacial lakes on the West Greenland ice-sheet margin. *Journal of Glaciology, 52*(179), 608-618. doi:10.3189/172756506781828386.

Porter, C., Morin, P., Howat, I. *et al.* (2018) *ArcticDEM*. doi:10.7910/DVN/OHHUKH. Harvard Dataverse, V1, July 20, 2021.

Shannon, S. R., Payne, A. J., Bartholomew, I. D. *et al.* (2013). Enhanced basal lubrication and the contribution of the Greenland ice sheet to future sea level rise. *PNAS*, *110*(35), 14156-14161. doi:10.1073/pnas.1212647110.

Snide, C. E., Gilbert, L., Meyer, A., Samson, P., Flanner, M., and Bassis, J. (2020). Seeing the Greenland Ice Sheet through students' eyes, *Eos, 101.* doi:10.1029/2020EO139739.

Xu, H. (2005). A study on information extraction of water body with the modified normalized difference water index (MNDWI). Journal of Remote Sensing. 9(5). 589-595.

Yang, K., Smith, L., Cooper, M., Pitcher, L., Van As, D., Lu, Y., *et al.* (2021). Seasonal evolution of supraglacial lakes and rivers on the southwest Greenland Ice Sheet. *Journal of Glaciology, 67*(264), 592-602. doi:10.1017/jog.2021.10.